Sedimentary Geology 222 (2009) 5–15

Contents lists available at ScienceDirect

Sedimentary Geology

journal homepage: www.elsevier.com/locate/sedgeo

High sedimentation rates in a karstic lake associated with hydrothermal turbid plumes (Lake Banyoles, Catalonia, NE Spain)

Marianna Soler *, Teresa Serra, Xavier Casamitjana, Jordi Colomer

Environmental Physics Group, Department of Physics, University of Girona, Spain

ARTICLE INFO

Keywords:
Hydrothermal plumes
Sediment transport
Sedimentation rates
Fluidisation
Groundwater input

ABSTRACT

In Lake Banyoles (northeastern Spain), warm water enters through lake bottom seeps and generates two hydrothermal turbid plumes. One of them is perennial in character and the other is active only after fluidisation events of the bottom sediment caused by reactivation of the bottom seeps after rainfall in the aquifer recharge area. The vertical development of both hydrothermal plumes is very sensitive to the thermal stratification of the water column. When a plume reaches a level of neutral buoyancy, a turbidity current spreads laterally and transports sediment particles across the lake. Silt particles transported by the plume are used in ADCP backscatter images to determine its maximum and equilibrium heights. Field results are compared and found to be in accordance with models for thermal convection from finite isolated sources. When the lake is stratified, the vertical transport of sediment is confined to the hypolimnion; when the lake water column is mixed, the plume reaches the surface of the lake. The turbidity current is usually confined to the southern sub-basin of the lake during stratification, resulting in higher sedimentation rates. During fluidisation events the sedimentation rates are one order of magnitude greater than in periods without fluidisation. For the fluidisation periods, turbidity has been estimated to be ~10 FTU.

1. Introduction

Convection from isolated sources has received much attention because of its application to geophysical and engineering flows. Relevant examples include plumes (continuous sources of buoyancy) and thermals (fixed volumes of buoyant fluid). Man-made plumes include waste in oceans and chimney stacks in the atmosphere (Turner, 1973; List, 1982). In devices that eject buoyant fluid with some momentum, the buoyancy becomes the dominant driving force as the flow evolves and can be defined as buoyant jets. Oceanic hydrothermal vents are an example of a natural flow driven by isolated buoyancy sources. They are formed in regions where upwelling magma from the Earth's interior solidifies on mid-ocean ridges to form new crust, thus transferring heat from the magma to the surrounding waters to create turbulent plumes (Lupton et al., 1985; Speer and Rona, 1989). Another phenomenon of geophysical interest is deep ocean convection, where predisposed regions of high-latitude oceans (known as “chimneys”) become unstable due to intense surface cooling and generate turbulent convection that can penetrate to depths of between 2 and 4 km (Fernando et al., 1998).

Whether and when deep convection occurs depends on the seasonal development of the surface buoyancy flux with respect to the initial stratification at the beginning of the winter period, and on the role of lateral advection (Marshall and Schott, 1999). In the open ocean the convective plumes entrain ambient fluid and, if deep enough, become affected by rotational effects and any pre-existing stratification. In shelf regions the convective plumes reach the sloping bottom, spread along it toward deeper locations, and are diverted by the Coriolis force where this applies.

Convection dynamics and flow features have also been studied in many laboratory and numerical experiments. Localised turbulent convection has been generated in laboratory tanks, for both laterally confined and unconfined domains issuing into a homogeneous, non-rotating environment (Kaimal et al., 1976; Boubnov and Van Heijst, 1994; Colomer et al., 1998a; Colomer et al., 1999) and into a homogeneous, rotating fluid (Maxworthy and Narimousa, 1994; Boubnov and Van Heijst, 1994; Dai et al., 1994; Narimousa, 1996; Whitehead et al., 1996, Narimousa, 1997; Jacobs and Ivey, 1998). These experiments have led to the prediction of a physical scaling of the convective chimney's length and velocity under gravity and rotation, with a resulting dependency on buoyancy, B_o, the Coriolis parameter, f, and the chimney length scale, h. As an alternative to laboratory experiments, localised open-ocean convection has been examined by high-resolution numerical models (Morton et al., 1956; Legg et al., 1996; Julien et al., 1999; Fannelop and Webber, 2003) to investigate the relationship between the convection process and the external

* Corresponding author. Environmental Physics Group, Department of Physics, University of Girona, Montilivi Campus, 17071, Girona, Spain. Tel.: +34 972 418 372; fax: +34 972 418 098.
E-mail address: marianna.soler@udg.edu (M. Soler).

0037-0738/$ – see front matter © 2009 Elsevier B.V. All rights reserved.
doi:10.1016/j.sedgeo.2009.07.006

parameters (Phillips, 1966; Okada et al., 2004). In addition, numerical experiments have allowed studies of the growth as well as the scaling laws of buoyant plumes (Speer and Marshall, 1995) and megaplumes (Lowell and Germanovich, 1995; Palmer and Ernst, 1998), and analysis of the rotation effect of the heat source (Leaman and Schott, 1991; Pham et al., 2006).

The convection process — the thermal plume — is generated by an underlying heat source. If the heating is confined to a finite area, a vertical thermal plume and associated circulation will develop as a result of the temperature (density) difference between the plume and its environment. The plume stops rising as the temperature difference between the plume and its surroundings decreases due to entrainment

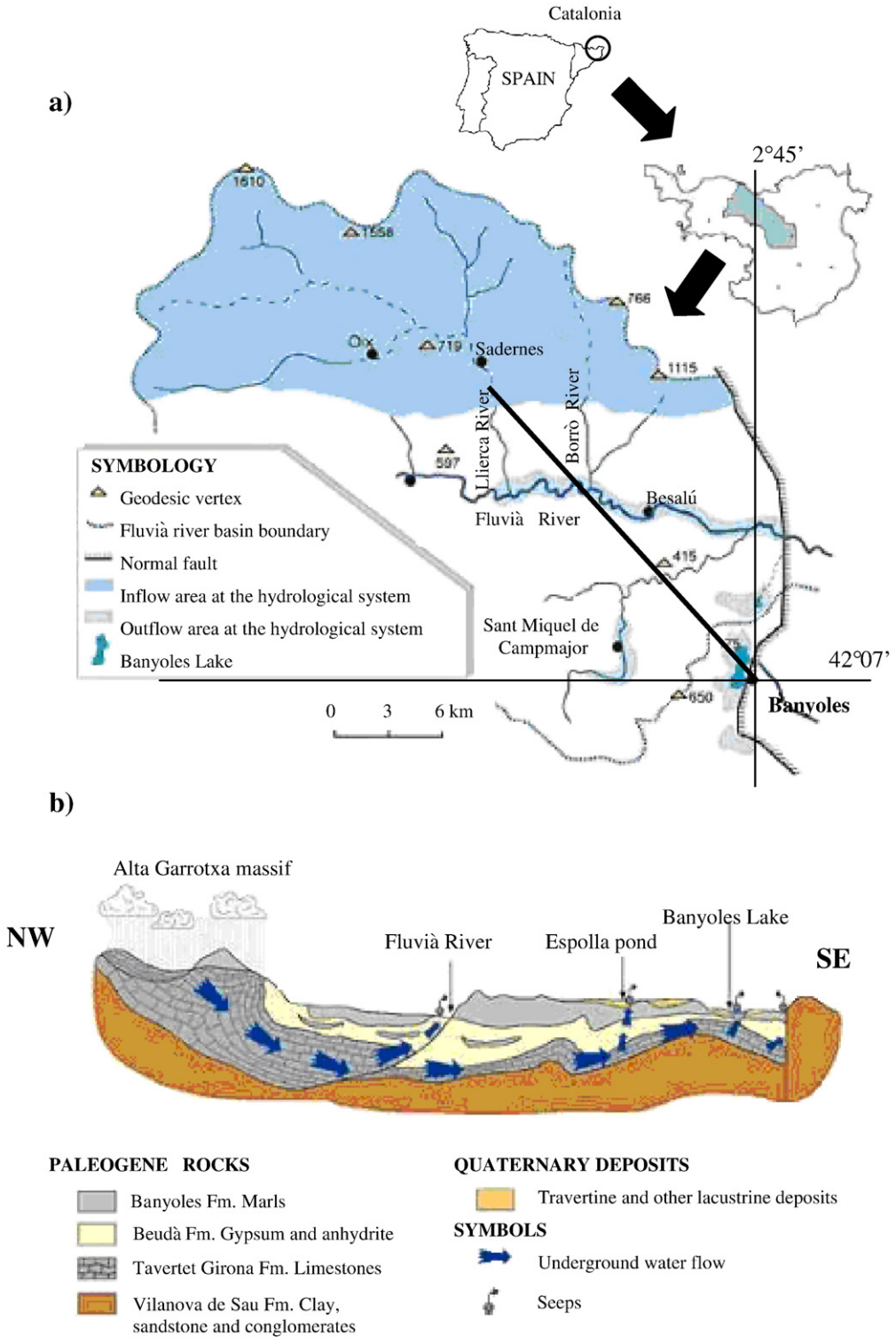

Fig. 1. a) Location of Lake Banyoles (Catalonia, northeastern Spain) and representation of the hydrological system in the Lake Banyoles region. The solid line shows the location of the cross section below. b) Path of the groundwater flow along the cross section marked at (a) (Sanz, 1985 redrawn by Brusi et al., 1992).

or to the intermixing of plume and ambient environment fluids. Therefore, the height/depth of a plume is determined by a balance between the strength and size of the heat source (Lu et al., 1997a,b) and the strength of the ambient stratification.

In Lake Banyoles (northeastern Spain; Fig. 1), warm water enters through lake bottom seeps related to several sublacustrine karstic sinks (Fig. 2). These seeps give rise to two hydrothermal turbid plumes. One of the plumes (related to sink B-1) is perennial while the other (related to sink B-2) is only active after fluidisation events. These events affect the bottom sediment when the sink seeps reactivate after rainfall in the aquifer recharge area. This study deals with detailed description of the horizontal and vertical extension of both hydrothermal plumes through measurements of ADCP back-scattering and sediment traps. The study was undertaken during a very active convective period in the lake sinks B1 and B2 (Fig. 2), when sediments in B2 were fluidised as a result of a period of high precipitation in the lake recharge area. The hydrothermal plumes of B1 and B2 were both active during this period and a large suspended concentration of sediments was present in the water column.

2. The Banyoles Lake System

2.1. Geological setting

The Lake Banyoles (NE Spain; 42°07′N, 2°45′ E) is a small (1.12 km^2) multi-basin lake that belongs to the Banyoles–Besalú lacustrine zone, in its turn located at the SW sector of L'Empordà basin. This sedimentary basin is located to the west of La Garrotxa zone and resulted from widespread neogene extension that developed at the Eastern Pyrenees. The NW–SE oriented faults that bound this basin affected the mainly E–W oriented alpine paleogene thrusts that make up this part of the Pyrenean range (Tassone et al., 1994; Saula et al., 1994 and references therein).

The substratum of the Lake Banyoles consists of thick paleogene successions that developed at the southern Pyrenean foreland basin, and include a variety of siliciclastic, evaporite and carbonate units (Serra-Kiel et al., 2003 and references therein; see legend in Fig. 1b). The Lake Banyoles was originated in relation to tectonic-karstic processes and mainly developed as a consequence of the water infilling of coalescent karstic sinkholes affecting the subsurface evaporite units (i.e., Beudà Formation; Fig. 1b).

2.2. The Lake Banyoles basin

The lake can be split into two (northern and a southern) sub-basins separated by a shallow sill. In its turn both sub-basins are composed of six small subaqueous karstic sinks (B1–B6, shown in Fig. 2a). Sinks B1 and B2 are the largest and deepest (73.5 m and 77 m respectively; Canals et al., 1990) and are situated in the southern lacustrine sub-basin with the remaining four in the northern sub-basin. The main supply of water to the lake is through subterranean seeps at the bottom of the sinks (Abella, 1980; Casamitjana and Roget, 1993; Colomer et al., 1998b). An underlying fault that is located at the eastern end of the lake (Fig. 1) and acts as a barrier to groundwater movement in a complex series of confined aquifers, forces the vertical discharge of the groundwater flow through the bottom of the sinks (Moreno-Amich and Garcia-Berthou, 1989). The aquifers are supplied by precipitation in two watersheds, located between 15 and 40 km to the northwest of Banyoles (Sanz, 1985). Groundwater flow is mainly through B1, which supplies 500 L s^{-1} or 85% of the lake's total incoming water (Roget and Casamitjana, 1987). The volume discharged by several creeks on the western shore of the lake is much smaller and depends on seasonal variations (Casamitjana et al., 1988; Roget et al., 1994; Colomer et al., 1998a,b). As a result of cumulative episodes of active karstic collapses affecting the paleogene evaporites,

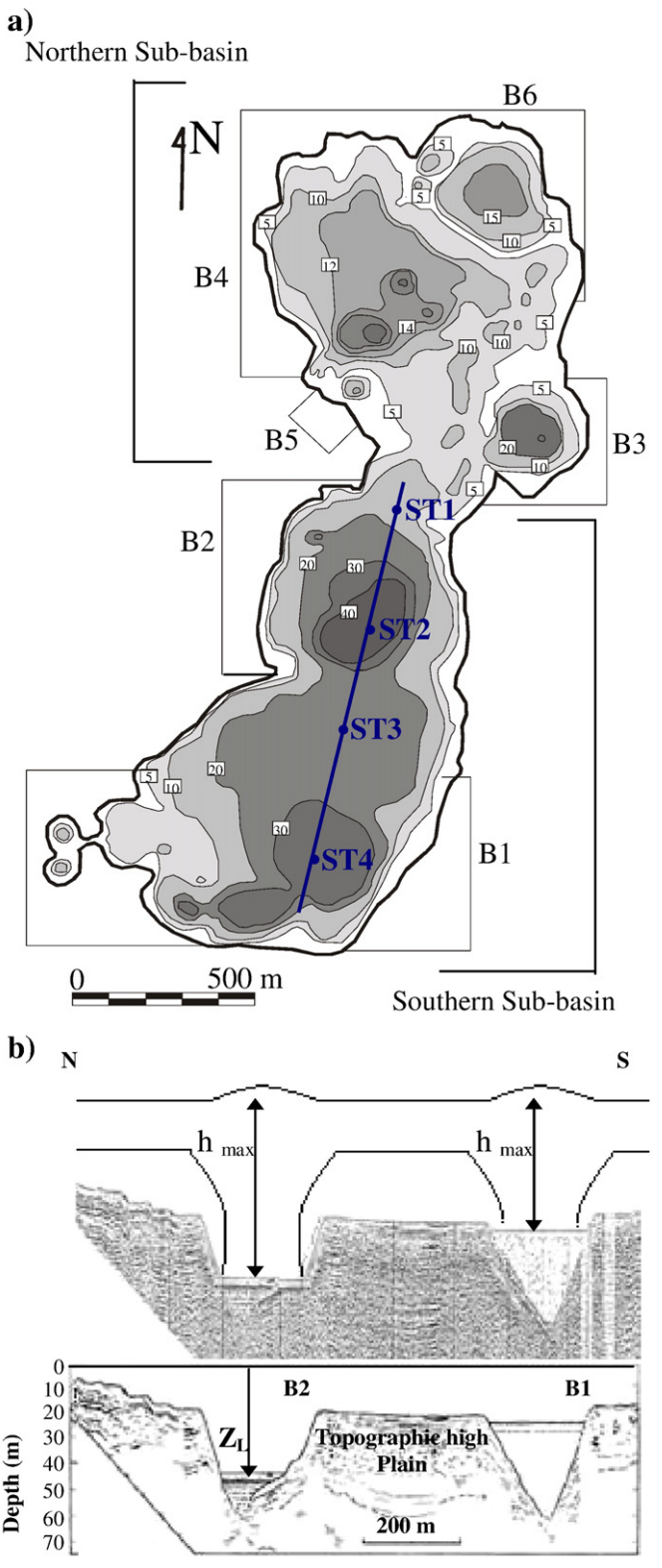

Fig. 2. a) Bathymetric map of Lake Banyoles constructed from echo-sounding profiles (Moreno-Amich and Garcia-Berthou, 1989). The lake is divided into two main sub-basins in its turn split into six smaller karstic sinks. The solid line defines the north–south transect along the location of the four stations (ST1–ST4). b) (top) North–south seismic transect with a schematic view of the hydrothermal plumes at B1 and B2. The plumes end at height h_{max}; (bottom) a graphic interpretation of the section from B2 to B1 (Canals et al., 1990). The seismic profile clearly shows the lutocline located at a depth Z_L from the surface.

the most recent of which was in 1978 (Julià, 1980), all the sinks are cone-like bottom depressions (Fig. 2b).

The subterranean seeps mix up the sediments above them into a fairly sharp interface known as the lutocline which can be clearly detected by seismic profiling (Fig. 2b-top) and is located at a depth Z_L from the surface (Fig. 2b-bottom). During periods of high precipitation in the recharge area, the Alta Garrotxa Massif, the lutocline can migrate upward.

The mean mass concentration of the fluidised sediment layer in B1 ranges from 100 to 130 g/L, while the sediment concentration in B2 varies from 280 g/L at the beginning of a fluidisation event to 180 g/L as sediments remain in suspension (Colomer et al., 2002). As a result of fluidisation events, the particle volume concentration (PVC) of suspended sediment in the lake water column can raise up to 44 μL/L, which is from 8 to 29 times greater than the usual PVC values (Colomer et al., 2002).

2.3. Convection in the Lake Banyoles water column

The perennial hydrothermal plume located in the main subaqueous sink of the karstic Lake Banyoles (B-1, Fig. 2) was described for the first time by Colomer et al. (2001) in the same way that other convective phenomena were described previously (i.e., turbulent convective plumes from localised sources by Maxworthy, 1997; oceanic and atmospheric deep convection by Schott et al., 1993, 1996; atmospheric microbursts by Lundgren et al., 1992; and urban heat islands by Lu et al., 1997a,b). As much as 85% of the total underground inflow enters the lake through this sink (Roget et al., 1994). The temperature of the water at the lutocline level (a strong density gradient that divides the water column into two zones: a zone below, full of sediments in suspension, and a zone of clearer water above) is warmer (~19 °C, constant throughout the year) than the hypolimnetic water immediately above it, and this difference in temperature generates a convective hydrothermal plume. In contrast to ocean convection plumes, where the source of the convection is situated at the top of the water column and surface water cools and forms dense water, the source in Lake Banyoles is situated at the bottom of the lake, where warm water, rich in sediments, heats the hypolimnetic water and makes it less dense and therefore buoyant. The plume develops upwards and entrains particles from the lutocline up to an equilibrium depth (Casamitjana and Roget, 1993; Serra et al., 2002a). At the equilibrium depth, the water spreads laterally to form a mesopycnal turbidity current, in accordance with the classification of Mulder and Alexander (2001) for a volume sediment concentration <10%. This turbidity current is ~0.02 °C warmer than the surrounding water and has a typical thickness of ~1 m (Colomer et al., 2001). Sedimentation from turbidity currents and density interfaces has been found to be an effective mechanism for the transport of suspended material across the bottom of the water column, thereby influencing the bottom sedimentary records for the whole lake (Serra et al., 2005). This sedimentation process, at the southern sub-basin of the lake, has been attributed mainly to double diffusive sedimentation rather than to single particle suspension settle-out (Serra et al., 2002b; Zamora and Moreno-Amich, 2002). Sediments found at the southern sub-basin bottom consist of massive bioturbated light grey (10Y 7/2) carbonate lutites with rare interbedded thin light grey (7.5Y 7/1) layers. These muddy sediments contain abundant gas bubbles.

The vertical structure of the plume depends on the stratification of the water column, which in turn depends on seasonal meteorological conditions. During the stratified period of the lake, the plume is restricted to the hypolimnetic zone. At the beginning of the summer season the plume reaches the bottom of the metalimnion, but at the end of this season strong stratification overcomes plume buoyancy and it no longer reaches the bottom. During mixed phases of the lake, the plume develops in the entire water column and reaches the surface of the lake, where particles accumulate and spread around the centre (Serra et al., 2002a). The maximum height to which the sediment-entrained plume can rise is also affected by the formation of aggregates, ranging between 10 and 130 μm (Casamitjana et al., 1996).

During high precipitation periods in the recharge area, the aquifer water pressure increases enough to resuspend the confined sediments of sink B2 (see Fig. 1; Colomer et al., 2003); this resuspension results in a vertical displacement of the lutocline, ranging between ~5 and 20 m (Canals et al., 1990; Casamitjana and Roget, 1993; Colomer et al., 2002). The differences in the consolidation state of the sediments, in the different sinks and at different times, are caused by the precipitation in the recharge area; if it decreases, the groundwater discharge decreases and the sediments begin to consolidate. Conversely, an increase in groundwater discharge acts to disturb the sediments, and mix them into a zone of overlying water.

Records show that sediment fluidisation in sink B2 of the lake develops episodically (episodic fluidisation) as a function of the amount of rainfall in the recharge aquifer area (Colomer et al., 2002; Soler et al., 2007). Sediment fluidisation is of great limnological interest because it is a mechanism that carries particles in suspension from the sediment interface upward into the lake water column (Colomer et al., 1998b), which in turn affects water quality, fish distribution (Serra et al., 2002a), and the sedimentary records for the whole lake (Serra et al., 2005).

3. Techniques and material studied

In order to study convective dynamics in Lake Banyoles and their influence on sediment transport in the water column, several field surveys were carried out between October 2003 and November 2004. Measurements were taken weekly during the beginning of the fluidisation event, which lasted four months, and afterwards monthly measurements were taken for the rest of the survey. An acoustic Doppler currentmeter profiler (ADCP, RDI 600 kHz Workhorse Sentinel) was used to measure the three dimensional velocity (u, east–west, v, north–south and w, vertical) within the whole of the water column, of a transect along the main axis of the lake in the southern sub-basin (see solid line in Fig. 2a). Data from the ADCP were received from 45 depth bins, each a metre high, with the first at a depth of 3 m. The sampling rate was set at 1 Hz with the raw data processed to obtain 7.5 min of averaged data, with a standard deviation of 0.1 cm s^{-1}.

A conductivity–temperature–depth profiler (CTD SBE 19plus SEACAT, Sea Bird Instruments) was used to obtain accurate temperature measurements. Measurements were taken systematically at four stations along the main axis of the lake (Fig. 2a). The CTD-19plus samples at 4 Hz and profiles temperature with a range of −5 °C to 35 °C, an initial accuracy of 0.005 °C, and a resolution of 0.0001 °C, and depth (Strain-Gauge Pressure) with a range of 0 to 1000 m, an initial accuracy of 0.1%, and a resolution of 0.002% of full scale range. There is an auxiliary sensor for turbidity, which has a linearity deviation of less than 2%, from 0 to 750 FTU (Formazin Turbidity Units) and a sensitivity of 200 mV/FTU with a range of 25 FTU.

A laser *in situ* scattering and transmissometry probe (LISST-100, Sequoia Scientific, Inc.) was used to measure the particle size distribution patterns in the water column. The LISST-100 covers a measurable size range of 1.2 to 200 μm and also measures depth by means of a pressure sensor, with a resolution of 5 cm. Previous works (Traykovski et al., 1999; Serra et al., 2001) demonstrate that the LISST-100 is an appropriate instrument for estimating the concentration of suspended particles in a water body. Particle size distribution profiles were performed with a spatial resolution of 0.25 m.

Four sets of sediment traps (ST) consisting of structures containing four units of 20 mL glass tubs with an area-to-volume ratio of 5 (see details in Gacia and Duarte, 2001) were also deployed in October 2003, December 2003, and October 2004 at the four selected stations

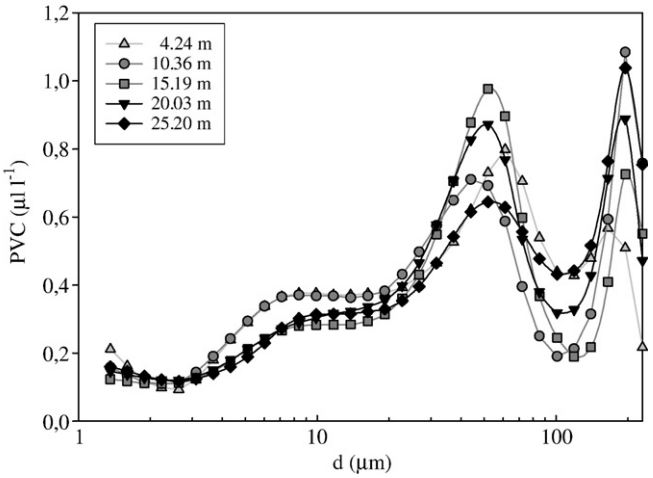

Fig. 3. Particle size distribution (PSD) of particles obtained at different depths of the water column at B1 on 10/22/2003. The PSD was measured with the LISST-100.

(Fig. 2a) and at three different depths depending on the water column stratification. Samples were filtered in glass-fibre filters, dried, and then heated in a muffle furnace at 500 °C (following the procedure used by Kristensen and Andersen, 1987).

4. Results and analysis

The particle size distribution (PSD) obtained throughout the water column (Fig. 3) presents a trimodal shape, with peaks centred at 8 µm, 50 µm, and 200 µm. The two smaller peaks are characteristic of a hydrothermal plume (Serra et al., 2002b) corresponding to fine silts (8 µm) and coarse silts (50 µm), and the larger one corresponds to aggregates of silt and clays and a few dead phytoplankton cells that have settled throughout the water column.

The laboratory analyses of the sediment collected during the surveys show a high percentage of inorganic matter in the whole of the water column (Fig. 4). The inorganic matter is fairly homogeneously distributed throughout the southern sub-basin. This is in contrast to the results found during previous surveys carried out between July 1998 and July 2000, when traps located closer to the source (sink B1) received higher particle sedimentation amounts (10–25 g m^{-2} d^{-1}) compared to those far from the plume source in B1 (<5 g m^{-2} d^{-1}) (Serra et al., 2002b). The sedimentation rates found at the four stations (ST1–ST4) of 156 g m^2 d^{-1} are nearly one order of magnitude higher than those obtained earlier in Lake Banyoles, and for example, larger than those obtained at the entrance of Lake Kinneret (10–35 g m^{-2} d^{-1}) as a result of the discharge of the Jordan River (Koren and Klein, 2000). This homogeneity of inorganic particles within the vertical profiles during the 2003/2004 campaign is attributable to the high level of activity of the perennial hydrothermal plume in sink B1 and the episodic plume in sink B2 (Colomer et al., 2002; Soler et al., 2007). A comparison of the inorganic percentage values from the 10/28/2003 field survey with the other two (12/29/2003 and 09/28/2004) (Fig. 4) reveals that the highest percentage of inorganic matter is found during the first deployment and decreases with time, in accordance with the fact that the first sediment deployment corresponds to the beginning of the fluidisation period in sink B2, and that in September 2004 the fluidisation phase had already finished. More remains of organic matter (detritus) were also found in the water column in September 2004 than in December 2003; this can be attributed to the settling of the algae population that develops when spring starts and lives in the epilimnion throughout the summer.

The convective process generated above the lutocline resuspends sediment particles (consisting of clay and silts), which are transported upwards by the plume. Sediments in hydrothermal plumes can be traced, revealing their vertical and horizontal distribution.

5. ADCP backscatter calibration

All the particle studies performed until now in Lake Banyoles have been done with data using the LISST-100. During the 2003 October survey, some profiles were taken with both instruments (the LISST-

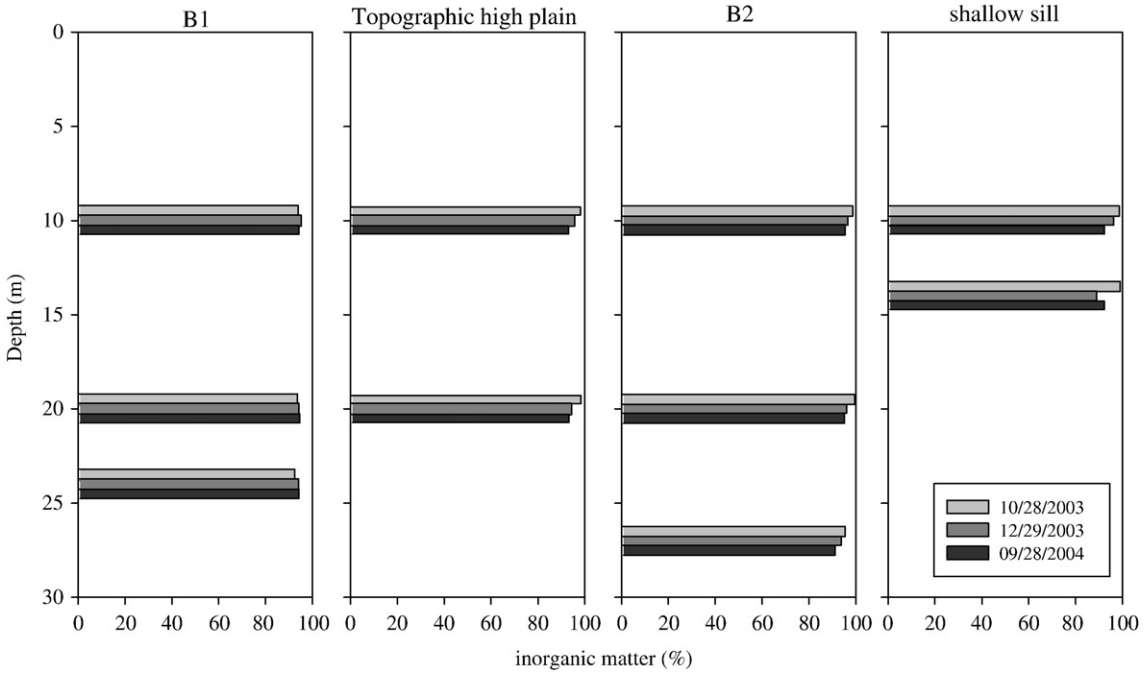

Fig. 4. Values of the percentage of inorganic matter from the sediment traps obtained at different depths of the water column at B1, B2, topographic high plain, and the shallow sill that divides the lake into two sub-basins (see Fig. 1a for details), for the days 10/28/2003, 12/29/2003, and 09/28/2004.

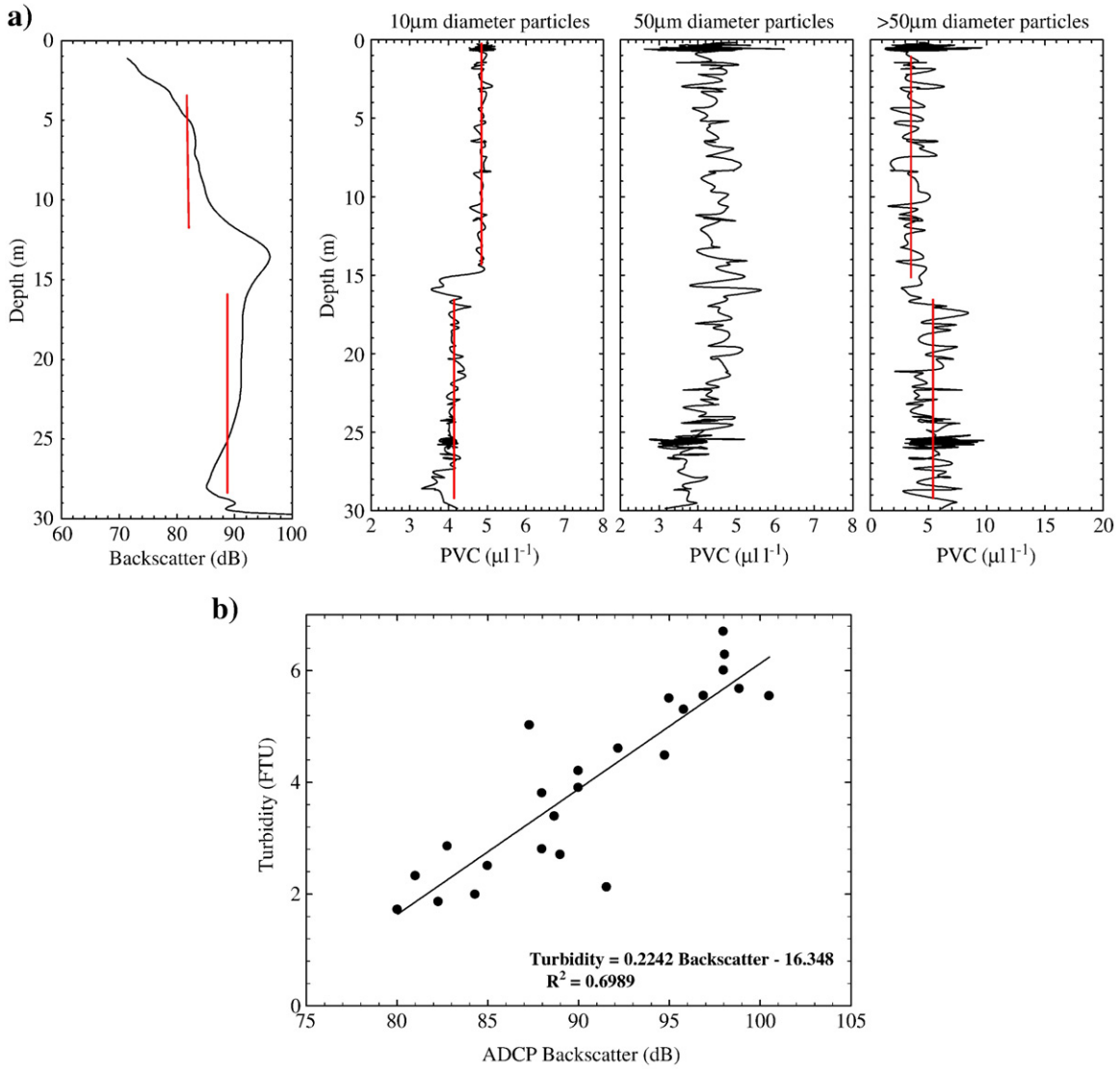

Fig. 5. a) Acoustic Doppler current profiler (ADCP) backscatter profile and particle volume concentration (PVC) of different diameter particles obtained with the LISST-100 in sink B1 on 10/22/2003. b) Regression line correlating ADCP backscattering to turbidity.

100 and the ADCP) to correlate the particle concentration with the backscatter signal. The ADCP frequency is 600 kHz, and hence the sensitivity to particle size is in the order of millimetres, so that the ADCP backscatter signal is also related to particle sizes in the order of millimetres. This pattern can change if there are many small particles, as what happens in the region within the hydrothermal plume in sink 2 (see Fig. 4). Although small particles (10 μm diameter) dominate, ADCP backscattering gives a stronger signal in the region where particles are larger than 50 μm in diameter. From the particle concentration profile two layers can be differentiated: the upper layer, from 0 to 15 m in depth, with a low particle concentration, and the lower layer, with a high level of particle concentration due to the presence of the hydrothermal plume. The ADCP thus measured an *in situ* two-dimensional image of particle distribution in the lake's water column, including the horizontal and the vertical extension (h_{max}, Fig. 2b) of the hydrothermal plumes.

In order to approximately quantify the concentration of particles in suspension in the water column, data from the ADCP backscatter (in dB — decibels) were correlated with the signal from a turbidimeter (in FTU) linked to the CTD (Fig. 5b), producing the following equation for the regression line: *turbidity* (FTU) = 0.22 *backscatter* (dB) − 16.35, with a R^2 value of 0.70.

ADCP measurements taken during the initiation of the fluidisation event in sink B2 in 2003 correspond to a value of ~10 FTU, which in turn corresponds to ~100 mg/L of suspended sediment concentration. This is the highest value found in Lake Banyoles. This value, in turn, coincides with the low range of the values found after a storm event in Caspar Creek Experimental Watershed, California (Lewis, 1996). Other studies have described the correlation between the particle concentration and the ADCP in order to study the turbidity of the lake through ADCP data (Bunt et al., 1999; Buckner, 2001).

6. Hydrothermal plume characteristics

Although many discharges into a water environment are classified as buoyant jets, they are derived from sources with both momentum and buoyancy. At the beginning, the initial flow is driven by the momentum of the fluid, but if the effluent is less dense than its surroundings, the resulting jet is influenced by buoyancy forces. Near the source, the flow is usually controlled entirely by the initial conditions, which include the geometry of the source, the outflow vertical velocity, and the initial temperature difference between the discharge and the ambient fluid. One of the primary variables

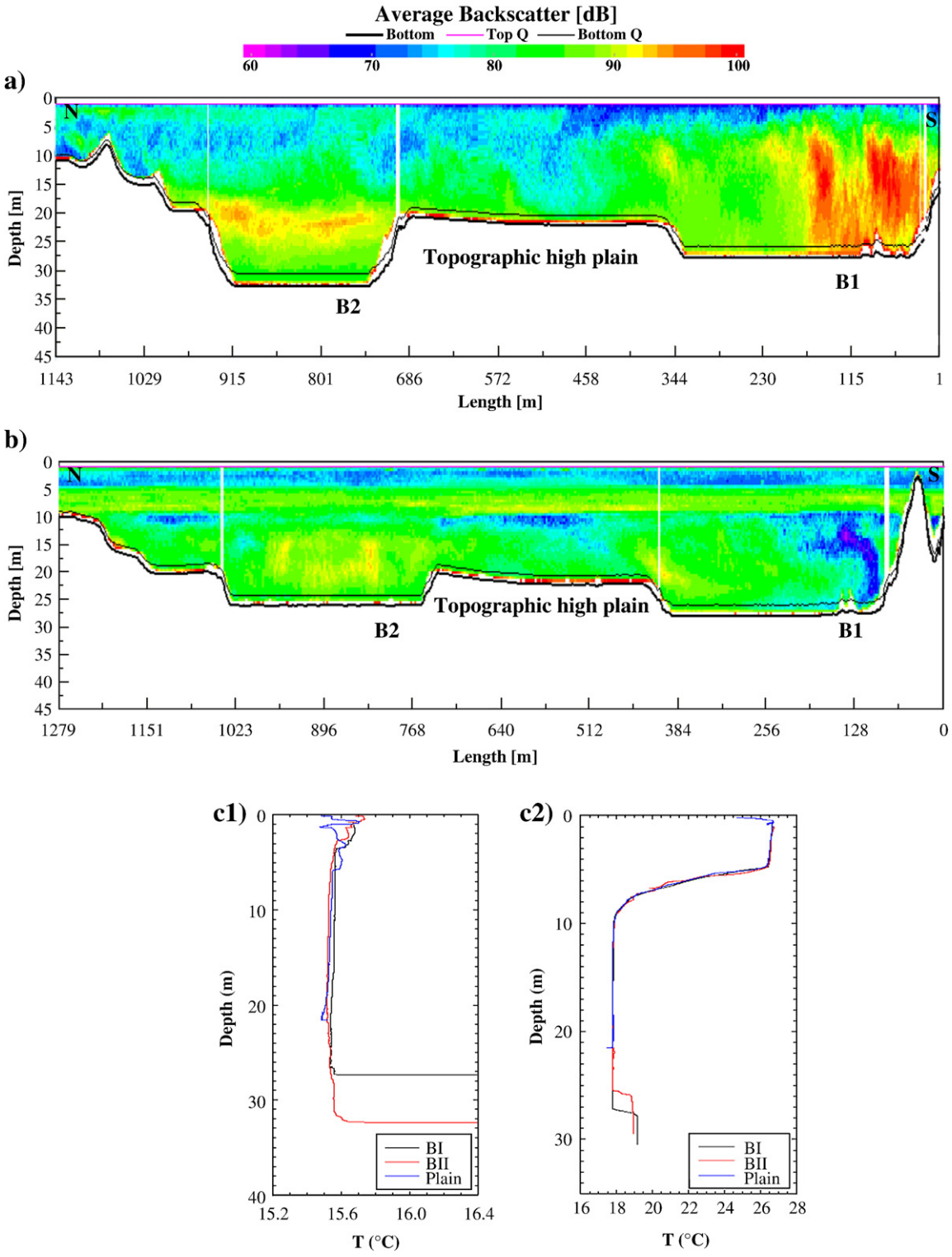

Fig. 6. ADCP backscatter transect along the southern sub-basin of Lake Banyoles on (a) 20 November 2003 — mixed period and (b) 5 August 2004 — stratified period; and temperature profiles (c1 and c2).

governing the dynamics of hydrothermal plumes is the buoyancy flux for a round source

$$B_o = g'_o w \quad (1)$$

where g_o' is the initial apparent gravitational acceleration, $g'_o = g\frac{\Delta\rho_o}{\rho}$, with $\Delta\rho_o$ as the difference between the density of the environment and the discharged fluid, and w is the mean outflow velocity, assumed to be uniform across the buoyancy source. In the fluidised period of the sediment mud, the upward velocity equals the particle settling velocity (as was first described by Roget and Casamitjana, 1987). In order to determine the settling velocity of sediments in B1 and B2, sediment samples were taken with Ruttner bottles below the lutocline in both sinks. Measurements were taken in the laboratory, by letting the sediments settle freely in a bottle, and recording the depth of the interface at different times, from which the settling velocity could be

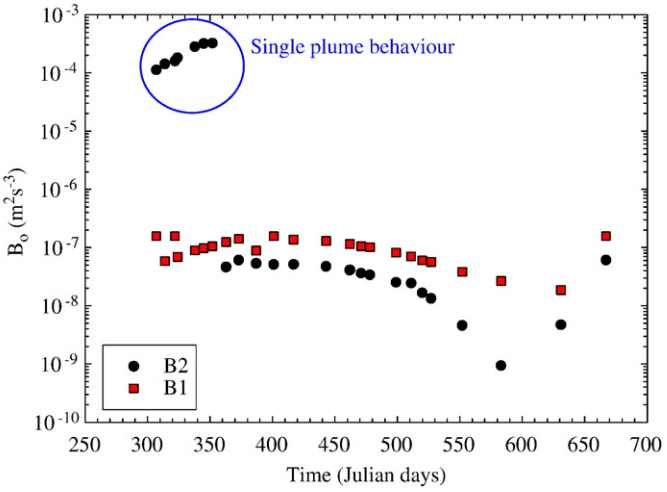

Fig. 7. Buoyancy flux value evolution in sinks B1 and B2 of Lake Banyoles, from October 2003 to November 2004.

estimated. A settling velocity of $v = (0.52 \pm 0.03) \cdot 10^{-5}$ m/s was measured for B2 and $v = (1.10 \pm 0.02) \cdot 10^{-5}$ m/s for B1 on September 2003.

Assuming that the input of unstable buoyancy flux at a surface or diameter D is balanced by the lateral removal of flux by eddies ejected out of the convective region, Whitehead et al. (1996) and Visbeck et al. (1996) were able to determine the vertical extension of the convection. Similarly, Colomer et al. (1998a,b) found that the depth of convection is determined by the inhibition of vertical growth due to the stratification of the water column. For both hypotheses, the maximum height to which a plume migrates has been found to be a function of the source diameter, D, the buoyancy flux per unit area, B_o, the Brünt–Väisäla frequency, N, which gives an idea of the stratification of the water column, and the independence of the rotation rate, f (Whitehead et al., 1996):

$$h_{max} = \frac{3.7(B_o D)^{1/3}}{N} \quad (2)$$

Also, to see the effect of stratification on the plume, it would be necessary to introduce the Richardson number, which is the ratio of the buoyancy force across the density interface to the inertia force:

$$\mathrm{Ri} = \frac{g_i' h_o}{(B_o R)^{2/3}} \quad (3)$$

where h_o is the depth of the convective layer and the apparent gravitational acceleration at the interface, and g_i' is calculated by the density difference caused by the temperature variation in the thermocline. This dimensionless number can be used to determine whether the plume will penetrate through the thermocline or not (Narimousa, 1996). The critical Richardson number is: $\mathrm{Ri_c} \sim 11$. Above this, it has been found that convective flows do not penetrate through density interfaces but propagate radially along the base of the mixed layer (Narimousa, 1996). In Lake Banyoles Richardson number values calculated during the study period were always higher than 11 ($26 < \mathrm{Ri} < 812$).

This means that although theoretical values of h_{max} (calculated using values of B_o (Eq. (1)) of the order of $\sim 10^{-7}$ m^2 s^{-3} and dependent on the period of the annual values of Brünt–Väisäla frequency between 0.001 $s^{-1} < N < 0.006$ s^{-1}) predicted a vertical extension of the plume up to the surface of the lake, the plume's depth was consistently found to be under the seasonal thermocline due to the strong effect of stratification overcoming the buoyancy effect.

7. Particle distribution

As shown in the temperature profiles (Fig. 6c1), at the end of October 2003 the lake begins to overturn. In sink B1, the temperature is nearly constant with depth, with a value of 15.55 °C at 27.5 m. At the lutocline upper boundary the temperature increases suddenly to 18.6 °C. In the plain (the area between basinal lows) the temperature is the same as in B2, and slightly colder (18.5 °C) than in B1.

As observed in Fig. 6a, the hydrothermal plume is fully developed in the southern part of sink B1, reaching the surface because the water column is mixed and there is no thermocline to limit its vertical development. In B1 the plume carries a maximum of particles corresponding to a turbidity value of ~10 FTU. From the backscattering signal, it can be observed that the plain is fairly clear of particles. In sink B2 the particle layer maximum is centred at a depth of 20 to 25 m.

Fig. 6c2 shows the entire water column in the stratified phase of the lake. The epilimnion layer is ~5 m, with a temperature of 25.5 °C; the thermocline occurs at a depth between 5 and 9 m and the hypolimnion has a constant value of 18 °C down to the bottom. In both cases, the thermocline acts as a barrier to the vertical development of the hydrothermal plumes. The maximum height observed in sink B2 is ~15 m, although using Eq. (2), a value of ~26 m was expected. The bottom of the thermocline starts at ~10 m where the hydrothermal plume collapses, in accordance with the Richardson number $\mathrm{Ri} = 807$ (Eq. (3)), which is above the critical value ($\mathrm{Ri_c} = 11$). Also, Fig. 6b shows the transport of sediment upward from the bottom of B2 by convection, which has overflowed the cone-like bottom sink and settled on the plain, corroborating the results of previous studies (Serra et al., 2005) to the effect that neither of the plumes penetrates the lake thermoclines for large Richardson numbers.

8. Development of sediment plumes within the lake

The onset of the fluidisation is characterised by episodic groundwater influx entering through preferential paths in the consolidated sediment at the bottom of B2. The water pressure through small diameter sources of the episodic plumes causes a high mean upward velocity, $w = 0.05$ m/s, a value three orders of magnitude greater than those found in the perennial plume of B1 (Fig. 7). These higher B_o values and the smaller ratio between the radius of the source in sink B2 and the height of the plume result in a regime called “single-plume convection” (Soler et al., 2008). After this, there is a transition period as the groundwater influx resuspends the settled sediment, where there is more than one preferential path, which causes the water pressure and vertical water velocity to decrease. Finally, when sediments are totally fluidised, the episodic hydrothermal plume of B1 resembles that of the perennial plume of B2.

Fig. 8a show the concordance between the model values of maximum plume height (dots) and the experimental values (crosses) measured by the ADCP backscatter signal seen in Fig. 6a and b.

During the stratified period, the maximum height of the plume obtained by the ADCP backscatter signal (crosses) coincides with the height of the seasonal thermocline. This shows that the thermocline acts as a barrier that prevents the plume from penetrating the upper layers of the lake.

Throughout the mixed period, the plume can develop freely within the entire column. Maximum height values of the plume found by open convection models give values greater than the lake's depth, indicating that the plume collapses at the surface in accordance with experimental data. Sometimes buoyancy is not strong enough and the plume does not reach the surface. This can be seen in the surveys carried out on 4 December and 18 December (corresponding to Julian days 338 and 352 respectively) (Fig. 8a). In this situation, the model prediction is in accordance with experimental results. It can also be seen that the time evolution of the lutocline (the sediment interface) is quite constant around a depth of 30 m.

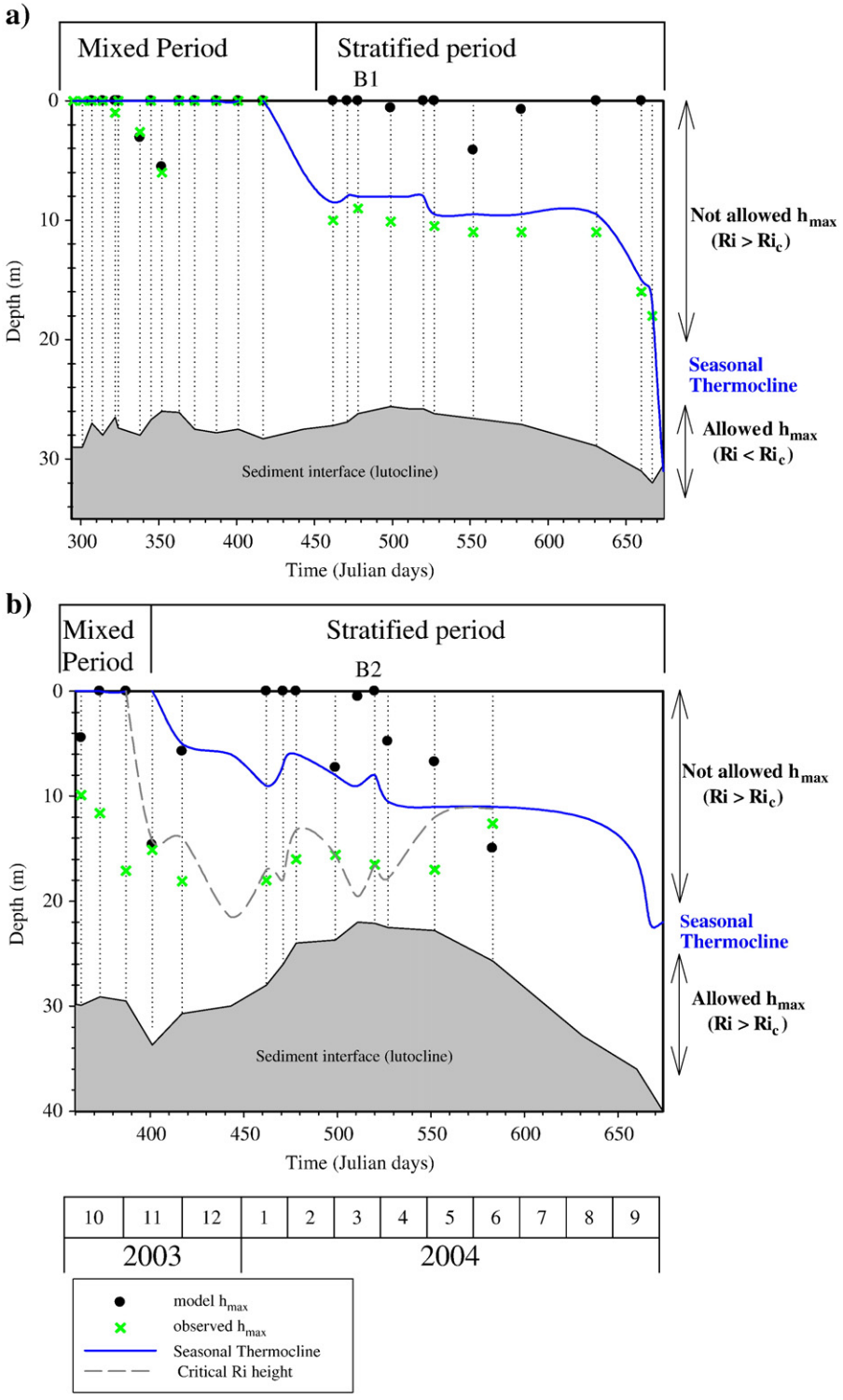

Fig. 8. Temporal evolution of the hydrothermal plume height in sinks B1 (a) and B2 (b) from 12/29/2003 to 05/08/2004. The grey area represents the vertical and time evolution of the lutocline. Each dotted line corresponds to a survey.

For the period when the episodic hydrothermal plume in sink B2 behaves like the perennial hydrothermal plume in sink B1, we can compare the experimental values of h_{max} (crosses in Fig. 8b) with h_{max} values determined by the conceptual model (dots in Fig. 8b). During the stratified period, the plume height experimental values should collapse at the thermocline as was found in B1, but as can be seen in Fig. 8b, this did not happen. Maximum plume heights found in sink B2 are limited not by the seasonal thermocline (solid line) but by any level of thermal stratification at which Ri = 11. Accordingly, the height at which the Richardson number reaches its critical value has been calculated (dashed line in Fig. 8b) and found to coincide in each survey with the experimental value (crosses). In sink B2 the evolution of the lutocline through time varies a lot; during the fluidisation period the interface of sediment-laden water can reach a depth of ~21 m, but subsequently it can sink to ~40 m.

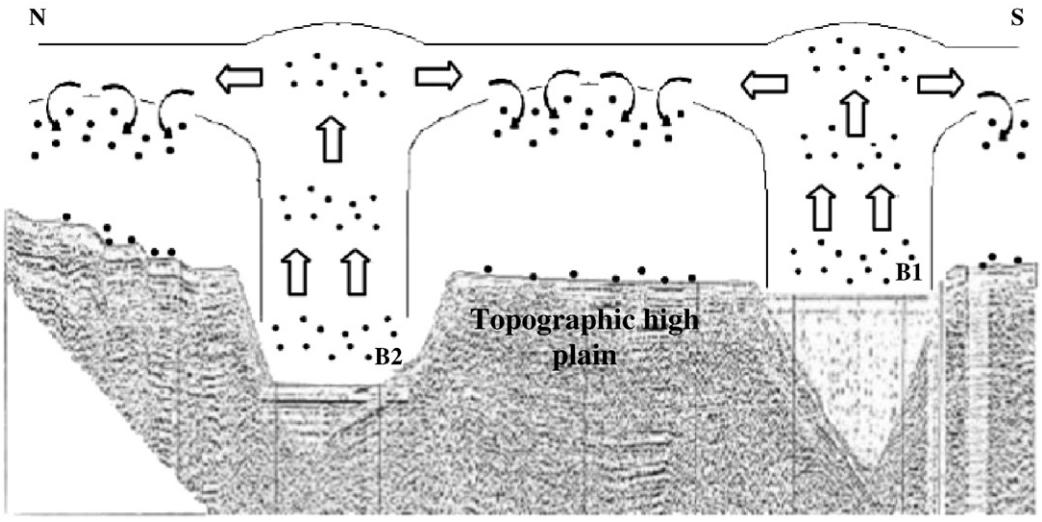

Fig. 9. Conceptual model of the sedimentation process in the southern sub-basin of Lake Banyoles. Clay and silt spread laterally and settle from a turbidity current that develops at the equilibrium depth of the hydrothermal plumes generated in both sinks, B1 and B2, during high precipitation periods.

9. Conclusions

Hydrothermal activity in Lake Banyoles resuspends particles in the water column. The episodic hydrothermal plume that develops in sink B2 is very sensitive to low temperature gradients, limiting its vertical dimension to levels below the seasonal thermocline. This limitation by the stratification of the water column results in different sedimentation rates along the southern lake sub-basin, depending on the season. When the hydrothermal plume in sink B2 is fully developed, a large quantity of sediment is transported upwards from the lutocline, resulting in an increase in sedimentation rates ($\sim$156 g m^{-2} d^{-1}) an order of magnitude higher than those for periods without fluidisation and with only the hydrothermal plume of B1 remaining active. As both sub-basins of the lake are separated by a shallow sill, sedimentary particles are restricted to the southern sub-basin during the stratification period, whereas in the mixed period particles reach the surface of the lake, where they spread laterally and can travel throughout the lake, subsequently settling across the whole of the lake bottom. We can summarise the results (see Fig. 9) using a conceptual model in which sediment-laden plumes generated in B1 (perennial plume) and in B2 (eventual plume, generated during high precipitation periods) transport clay and silt particles up the water column. Vertical plume development is restricted by the thermal stratification of the lake. During the stratified period, there is inhibition of vertical growth and clay and silt spread laterally and settle from a turbidity current that develops at equilibrium depth along the southern sub-basin of the lake.

Acknowledgement

The authors are grateful to Captain Joan Corominas for his outstanding help and support in this project.

References

Abella, C.A., 1980. Dinámica poblacional comparada de bacterias fotosintéticas planctónicas. Ph.D. Thesis, U.A.B., Bellaterra, Spain.
Boubnov, B.M., Van Heijst, G.F.V., 1994. Experiments on convection from a horizontal plate with and without background rotation. Exp. Fluids 16, 155–164.
Buckner, E., 2001. A comparison of the sediment flux in the channel and shoals of the estuarine turbidity maximum region of the Chesapeake Bay. VIMS 2001 Governor's School Final Report. 24 pp.
Bunt, J.A.C., Larcombe, P., Jago, C.F., 1999. Quantifying the response of optical backscatter devices and transmissometers to variations in suspended particulate matter. Cont. Shelf Res. 19, 1199–1220.
Canals, M., Got, H., Julià, R., Serra, J., 1990. Solution-collapse depressions and suspensates in the limnocrenic lake of Banyoles (NE Spain). Earth Surf. Process. Landf. 15, 243–254.
Casamitjana, X., Roget, E., 1993. Resuspension of sediment by focused groundwater in Lake Banyoles. Limnol. Oceanogr. 38 (3), 643–656.
Casamitjana, X., Roget, E., Jou, D., Llebot, J.E., 1988. Effect of the suspended sediment on the heating of Lake Banyoles. J. Geophys. Res. 93, 9332–9336.
Casamitjana, X., Colomer, J., Roget, E., Serra, T., 1996. On the presence of aggregates in the basin of Lake Banyoles. Geophys. Res. Lett. 23 (20), 2737–2740.
Colomer, J., Zieren, L.D., Fernando, H.J.S., 1998a. Comment on "Localized convection in rotating stratified fluid" by J. A. Whitehead et al. J. Geophys. Res. Oceans 103 (C6), 12891–12894.
Colomer, J., Ross, J.A., Casamitjana, X., 1998b. Sediment entrainment in karst basins. Aquat. Sci. 60, 338–358.
Colomer, J., Boubnov, B.M., Fernando, H.J.S., 1999. Turbulent convection from isolated sources. Dyn. Atmos. Oceans 30, 125–148.
Colomer, J., Serra, T., Piera, J., Roget, E., Casamitjana, X., 2001. Observations of a hydrothermal plume in a karstic lake. Limnol. Oceanogr. 46, 197–203.
Colomer, J., Serra, T., Soler, M., Casamitjana, X., 2002. Sediment fluidisation events in a lake caused by large monthly rainfalls. Geophys. Res. Lett. 29 (21). doi:10.1029/2001GL014299.
Colomer, J., Serra, T., Soler, M., Casamitjana, X., 2003. Hydrothermal plumes trapped by thermal stratification. Geophys. Res. Lett. 30 (21), 2092. doi:10.1029/2003GL018131.
Dai, Z., Tseng, L.K., Faeth, G.M., 1994. Structure of round, fully developed, buoyant turbulent plume. J. Heat Transfer 116, 409–417.
Fannelop, T.K., Webber, D.M., 2003. On buoyant plumes rising from area sources in a calm environment. J. Fluid Mech. 497, 319–334.
Fernando, H.J.S., Chen, R-r., Ayotte, B.A., 1998. Development of a point plume in the presence of background rotation. Phys. Fluids 10 (9), 2369–2383.
Gacia, E., Duarte, C.M., 2001. Elucidating sediment retention by seagrasses: sediment deposition and resuspension in a Mediterranean (*Posidonia oceanica*) meadow. Est. Coast. Shelf Sci. 52, 505–514.
Jacobs, P., Ivey, G.N., 1998. The influence of rotation on shelf convection. J. Fluid Mech. 369, 23–48.
Julià, R., 1980. La conca lacustre de Banyoles-Besalú. Ph. D. Thesis, U.A.B., Centre d'Estudis Comarcals de Banyoles, Banyoles, Spain.
Julien, K., Leff, S., McWilliams, J., Werne, J., 1999. Plumes in rotating convection. Part 1. Ensemble statistics and dynamical balances. J. Fluid Mech. 391, 151–187.
Kaimal, J.C., Wyngaard, J.C., Haugen, D.A., Coté, O.R., Izumi, Y., Caughey, S.J., Readings, C.J., 1976. Turbulence structure in the convective boundary layer. J. Atmos. Sci. 33, 2152–2169.
Koren, N., Klein, M., 2000. Rate of sedimentation in Lake Kinneret, Israel: spatial and temporal variations. Earth Surf. Process. Landf. 25, 895–904.
Kristensen, E., Andersen, F., 1987. Determination of organic carbon in marine sediments: a comparison of two CHN-analyser methods. J. Exp. Mar. Biol. Ecol. 109, 15–23.
Leaman, K.D., Schott, F.A., 1991. Hydrographic structure of the convection regime in the Gulf of Lions: Winter 1987. J. Phys. Oceanogr. 21, 575–597.
Legg, S., Jones, H., Visbeck, M., 1996. A heton perspective of baroclinic eddy transfer in localized open ocean convection. J. Phys. Oceanogr. 26, 2251–2266.
Lewis, J., 1996. Turbidity-controlled suspended sediment sampling for runoff-event load estimation. Water Resour. Res. 32 (7), 2299–2310.
List, E.J., 1982. Turbulent jets and plumes. Annu. Rev. Fluid Mech. 14, 189–212.
Lowell, R.P., Germanovich, L.N., 1995. Dike injection and the formation of megaplumes at ocean ridges. Science 269, 1804–1807.
Lu, J., Arya, S.P., Snyder, W.H., Lawson, R.E., 1997a. A laboratory study of the urban heat island in a calm and stably stratified environment. Part I: temperature field. J. Appl. Meteorol. 36 (10), 1377–1391.

Lu, J., Arya, S.P., Snyder, W.H., Lawson, R.E., 1997b. A laboratory study of the urban heat island in a calm and stably stratified environment. Part II: velocity field. J. Appl. Meteorol. 36 (10), 1392–1402.
Lundgren, T.S., Yao, J., Mansour, N.N., 1992. Microburst modelling and scaling. J. Fluid Mech. 239, 461–488.
Lupton, J.E., Delaney, J.R., Johnson, H.P., Tivey, M.K., 1985. Entrainment and vertical transport of deep-ocean water by buoyant hydrothermal plumes. Nature 316, 621–623.
Marshall, J., Schott, F., 1999. Open-ocean convection: observations, theory, and models. Rev. Geophys. 37 (1), 1–64.
Maxworthy, T., 1997. Convection into domains with open boundaries. Annu. Rev. Fluid Mech. 29, 327–371.
Maxworthy, T., Narimousa, S., 1994. Unsteady, turbulent convection into a homogeneous, rotating fluid, with oceanographic applications. J. Phys. Oceanogr. 24, 865–887.
Moreno-Amich, R., Garcia-Berthou, E., 1989. A new bathymetric map based on echosounding and morphological characterization of the Lake Banyoles. Hydrobiologia 185, 83–90.
Morton, B.R., Taylor, G., Turner, J.S., 1956. Turbulent gravitational convection from maintained and instantaneous sources. Proc. R. Soc. London, Ser. A 234, 1–32.
Mulder, T., Alexander, J., 2001. The physical character of subaqueous sedimentary density flows and their deposits. Sedimentology 48, 269–299.
Narimousa, S., 1996. Penetrative turbulent convection into a rotating two-layer fluid. J. Fluid Mech. 321, 299–313.
Narimousa, S., 1997. Dynamics of mesoscale vortices generated by turbulent convection at large aspect ratios. J. Geophys. Res. 5615–5624.
Okada, N., Ikeda, M., Minobe, S., 2004. Numerical experiments of isolated convection under polynya. J. Oceanogr. 60, 927–943.
Palmer, M.R., Ernst, G.G.J., 1998. Generation of hydrothermal megaplumes by cooling of pillow basalts at mid-ocean ridges. Nature 393, 643–647.
Pham, M.V., Plourde, F., Kim, S.D., Balachandar, S., 2006. Large-eddy simulation of a pure thermal plume under rotating conditions. Phys. Fluids 18 (1) doi:015101.1-015101.15.
Phillips, O.M., 1966. On turbulent convection currents and the circulation of the Red Sea. Deep-Sea Res. 13, 1149–1160.
Roget, E., Casamitjana, X., 1987. Balance hídrico del lago Banyoles. IV Congreso Español de Limnología. InUniversidad de Sevilla, Sevilla, Spain, pp. 39–46.
Roget, E., Casamitjana, X., Llebot, J.E., 1994. Calculation of the flow into a lake from underground springs using sedimentation rates. Neth. J. Aquat. Ecol. 28, 135–141.
Saula, E., Picart, J., Mató, E., Llenas, M., Losantos, M., Berástegui, X., Agustí, J., 1994. Evolución geodinámica de la fosa del Empordà y las Sierras Transversales. Acta Geol. Hisp. 29 (2–4), 55–75.
Sanz, M., 1985. Estudi Hidrogeològic de la Conca Banyoles-La Garrotxa. Quaderns del Centre d'Estudis Comarcals de Banyoles 1980–84, separata pp. 171–250. Redrawn by D. Brusi in Brusi, Maroto and Vila (1992) in "L'Estany de Banyoles" into "El Medi Natural de les Terres gironines" (Pallí i Brusi, eds.). Universitat de Girona. pp. 117–133.
Schott, F., Visbeck, M., Fischer, J., 1993. Observations of vertical currents and convection in the central Greenland Sea during the winter of 1988/89. J. Geophys. Res. 98, 14401–14421.
Schott, F., Visbeck, M., Send, U., Fischer, J., Stramma, L., Desaubies, Y., 1996. Observations of deep convection in the Gulf of Lions, Northern Mediterranean, during the winter of 1991/92. J. Geophys. Res. 26, 505–524.
Serra, T., Colomer, J., Cristina, X.P., Vila, X., Arellano, J.B., Casamitjana, X., 2001. Evaluation of a laser 'in situ' scattering system for measuring the concentration of phytoplankton, purple sulphur bacteria and suspended inorganic sediments in lakes. J. Environ. Eng. 11 (127), 123–130.
Serra, T., Colomer, J., Zamora, Ll., Moreno-Amich, R., Casamitjana, X., 2002a. Seasonal development of a turbid hydrothermal plume in a lake. Water Res. 36 (11), 2753–2760.
Serra, T., Colomer, J., Gacia, E., Soler, M., Casamitjana, X., 2002b. Effects of a hydrothermal plume on the sedimentation rates in a karstic lake. Geophys. Res. Lett. (ISSN: 0094-8276) 29 (21), 25–28.
Serra, T., Colomer, J., Julià, R., Soler, M., Casamitjana, X., 2005. Behaviour and dynamics of a hydrothermal plume in Lake Banyoles, Catalonia. Sedimentology 52 (4), 795–805.
Serra-Kiel, J., Travé, A., Mató, E., Saula, E., Fernández-Cañadell, C., Busquets, P., Tosquella, J., Vergés, J., 2003. Marine and Transitional Middle/Upper Eocene Units of the South-eastern Pyrenean Foreland Basin (NE Spain)). Geol. Acta 1 (2), 177–200.
Soler, M., Serra, T., Colomer, J., Romero, R., 2007. Anomalous rainfall and associated atmospheric circulation in the north-east Spanish Mediterranean area and its relationship to sediment fluidisation events in a lake. Water Resour. Res. 43, W01404. doi:10.1029/2005WR004810.
Soler, M., Serra, T., Colomer, J., 2008. Scaling analysis of single-plume convection from a hydrothermal source. J. Geophys. Res. 113, C05012. doi:10.1029/2006JC004073.
Speer, K.G., Rona, P.A., 1989. A model of an Atlantic and Pacific hydrothermal plume. J. Geophys. Res. 94, 6213–6220.
Speer, K.G., Marshall, J., 1995. The growth of convective plumes at sea floor hot springs. J. Mar. Res. 53, 1025–1057.
Tassone, A., Roca, E., Muñoz, J.A., Cabrera, L., Canals, M., 1994. Evolución del sector septentrional del margen continental catalán durante el Cenozoico. Acta Geol. Hisp. 29 (2–4), 3–7.
Traykovski, P., Latter, R.J., Irish, J.D., 1999. A laboratory evaluation of the laser in situ scattering and transmissometry instrument using natural sediments. Mar. Geol. 159, 355–367.
Turner, J.S., 1973. Buoyancy Effects in Fluids. Cambridge University Press, New York, USA.
Visbeck, M., Marshall, J., Jones, H., 1996. Dynamics of isolated convective regions in the ocean. J. Geophys. Res. 26, 1721–1731.
Whitehead, J.A., Marshall, J., Hufford, G.E., 1996. Localized convection in rotating stratified fluid. J. Geophys. Res. 101 (C11), 25705–25721.
Zamora, L., Moreno-Amich, R., 2002. Quantifying the activity and movement of perch in a temperate lake by integrating acoustic telemetry and a geographic information system. Hydrobiologia 483 (1–3), 209–218.